JOURNAL OF MATERIALS SCIENCE 28 (1993) 4615–4622

# The influence of alloy composition on microstructure and tensile behaviour of copper–lead alloys

S. ANAND, T. S. SRIVATSAN
*Department of Mechanical Engineering, The University of Akron, Akron, OH 44325, USA*
T. S. SUDARSHAN
*Materials Modification Inc., 2929-P1, Eskridge Center, Fairfax, VA 22031, USA*

Lead is a soft metal that possesses excellent antifriction and lubricating characteristics and is a desired addition to alloys which find use in friction-critical and low-load-bearing applications. The influence of alloy composition on microstructure, tensile properties and quasi-static fracture behaviour has been studied. Alloy composition, that is, lead content, was observed to have an influence on the size and distribution of lead globules in the copper matrix. The yield strength, ultimate tensile strength and elastic modulus of the alloy decreased with increase in lead content. The ductility of the alloys showed an improvement with increase in lead content. The influence of lead content on quasi-static fracture is discussed in detail.

## 1. Introduction

Lead is a metal that can be used in large quantities as a solid lubricant in many low-load rotating applications. It has excellent antifriction and lubricating characteristics on account of its excellent shear strength. However, because of its intrinsic softness and low melting point [1–3], it cannot be used alone and must be blended with hard metals in order that it can find use and application in modern engineering machinery. Consequently, it finds use in many types of bearings and also an alloying addition to improve the machinability and deep drawing characteristics of many complex alloys. Although lead mixes and blends well with hard metals in the liquid state, it tends to segregate upon cooling and solidification. Copper, which is harder than lead but softer than steel, is a good conductor and serves as an excellent matrix for lead. However, conventional metal processing techniques inhibit the formation of hard metal–lead mixtures in ratios exceeding 10 % Pb, due to problems of immiscibility. The metals mix well in the liquid state but segregate during the solidification process. Lead also has a tendency to segregate rapidly upon the application of heat due to its very low melting point [2–6].

In recent years, the discovery of new copper-containing alloys has resulted from the development and emergence of novel processing techniques which can solve the problem of immiscibility of lead in various hard metals and also produce a stable and homogeneous structure. Furthermore, the processing techniques have helped in the creation of an affinity, and thereby, improving the overall stability between the two elements. The emergence of these alloys has created considerable scientific and technological interest. However, only few studies have been conducted to understand systematically the role of alloy composition and microstructural effects on mechanical behaviour [8–11].

The present study was undertaken with the objective of documenting the influence of alloy composition, that is, lead content in a copper matrix, on microstructure, tensile properties and quasi-static fracture behaviour of copper–lead alloys. This study provides the basis for a more comprehensive study on the influence of alloy chemistry, that is, lead content on cyclic stress response, cyclic strain resistance and fracture behaviour of these alloys.

## 2. Experimental procedure

The copper–lead alloys used in this study were obtained in the form of 76 mm diameter ingots. Three alloys with different lead contents were provided. Copper and lead are the two primary ingredients of each alloy. The different lead contents used were 10, 25 and 40 wt %. The alloys were provided by Materials Modification Inc., and produced at the Western Reserve Manufacturing Co., Inc. foundry in Lorain, OH, USA.

The alloys were processed using a patented swirl die and an induction furnace. The alloys were melted and heated up to 1400 °C, then a mixture of proprietary additives that help to lower the surface tension of the melt and cause a vigorous reaction in the bath was added. After a hold time of about 2 min the metal was cast using a continuous caster. The swirl die facilitates the molten metal to swirl and mix uniformly at the point of exit, thereby, leading to extremely fine microstructures. The cooling rate was controlled by ensuring that a jet of cold recirculated and filtered water

0022–2461 

was injected just at the exit point of the die. Three different compositions of copper–lead alloys were produced and the processing and draw conditions in the continuous caster were identical for all three alloys.

Metallographic samples were cut from all the as-received alloys. The samples were mounted in bakelite, wet ground on 320, 400 and 600 grit silicon carbide paper using water as lubricant and then mechanically polished with 1 μm alumina-based polishing compound. Grain morphology and other intrinsic microstructural features were revealed using an etchant mixture of 100 ml doubly distilled water, 25 ml hydrochloric acid (HCl) and 25 g ferric chloride ($FeCl_3$). The resultant etched microstructures were observed in an optical microscope and photographed using standard bright-field technique.

Cylindrical specimens conforming to ASTM E8 specifications, with threaded ends, were machined from each alloy ingot. The specimens were smooth and cylindrical in the gauge section which measured 25 mm long and 6.35 mm diameter. The gauge sections of the test specimens were ground with 600 grit silicon carbide paper to remove any and all circumferential scratches and machine marks. Tensile stress–strain tests were performed at ambient temperature and in laboratory air environment (relative humidity 55 %). The specimens were deformed to failure in a computer-controlled servohydraulic test machine at a constant strain rate of $10^{-4}s^{-1}$. The axial strain was measured using a 12.7 mm gauge length extensometer fixed to the gauge section of the test specimen.

Fracture surfaces of the deformed tensile specimens were examined in a scanning electron microscope (SEM), to determine the predominant fracture mode and to characterize the fine-scale fracture features. Samples for SEM observation were obtained by sectioning parallel to the fracture surface.

## 3. Results and discussion

The optical microstructure of the as-received copper–lead alloy (denoted 9010, 90 wt % Cu–10 wt % Pb; 7525, 75 wt % Cu–25 wt % Pb; 6040, 60 wt % Cu–40 wt % Pb) is shown in Figs 1–3. The microstructure of the 9010 alloy consisted of very fine particles or globules of lead dispersed randomly in the copper matrix. The morphology of the dispersed lead particles was fairly well defined. The microstructure of the 7525 alloy revealed a larger number of dispersed lead particles than the 9010 counterpart. Furthermore, the particles of lead in the 7525 alloy were larger in size, with a resultant decrease in spacing between the particles. On account of randomness in both size and distribution, no attempt was made to measure the volume fraction of lead particles or the interparticle spacing.

The 6040 alloy revealed a microstructure comprising uniformly large lead particles dispersed in the copper matrix. Finer globules of lead were dispersed

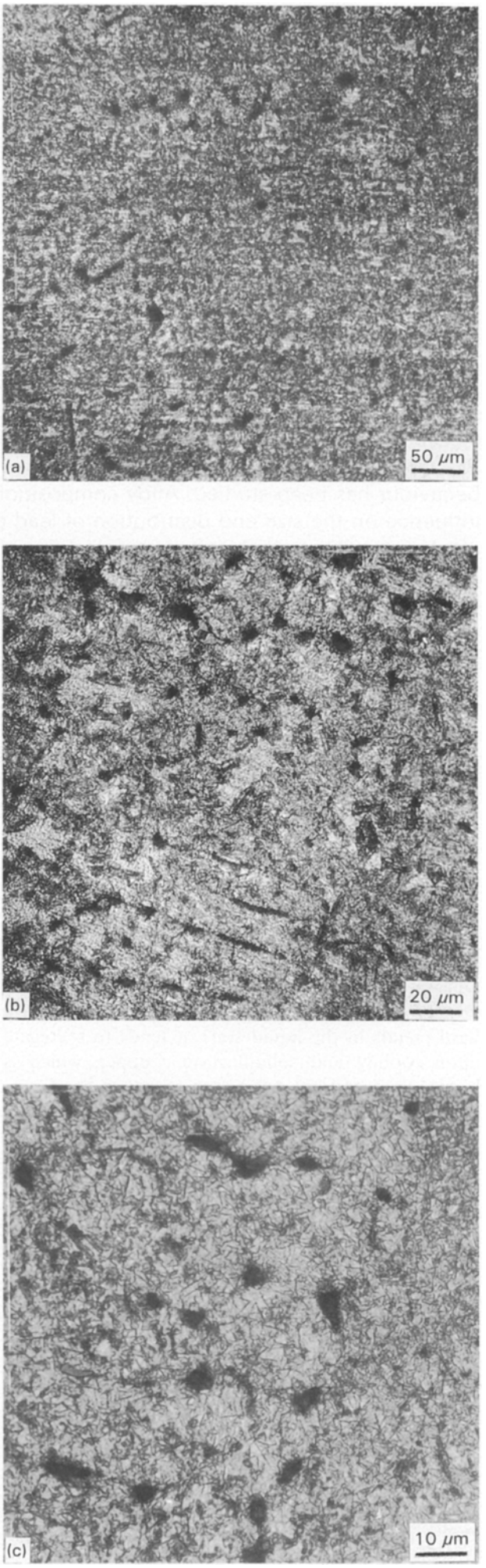


*Figure 1* Optical micrograph of the copper (90 wt %)–lead (10 wt %) alloy showing distribution of lead particles in the copper matrix.

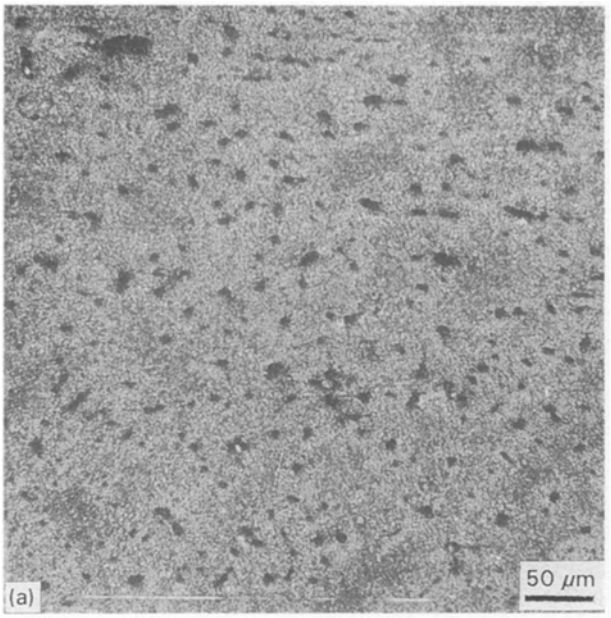


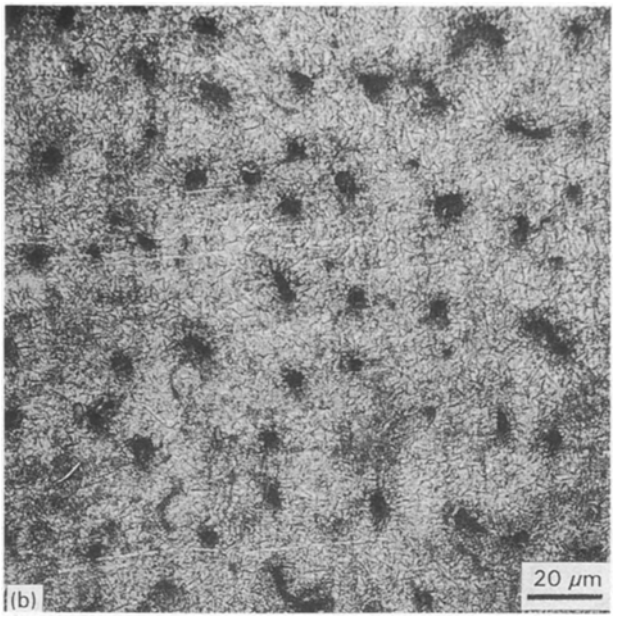


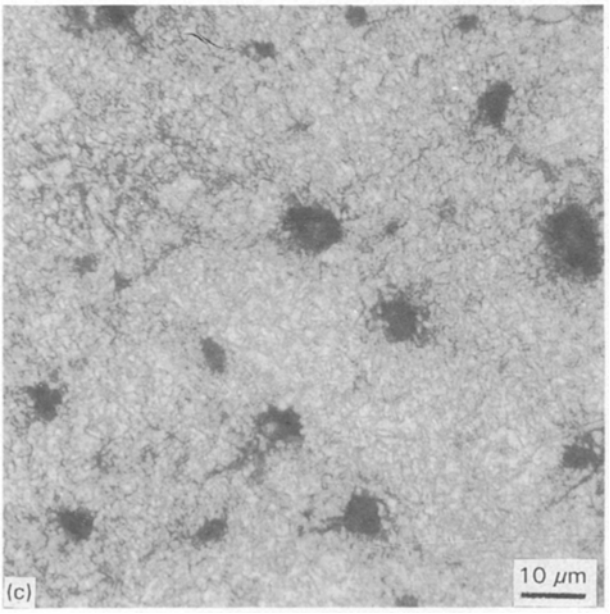


*Figure 2* Optical micrographs of the copper (75 wt %)–lead (25 wt %) alloy showing distribution of lead particles in the copper matrix.

between the larger particles. This microstructure revealed a decrease in interparticle spacing between the dispersed lead particles. The composite copper–lead matrix, for all three alloys, exhibited fine grains. The grains were not clearly resolvable in the optical microscope. Variation of lead content was found to have little influence on microstructure of the matrix.

### 3.1. Tensile properties and fracture behaviour

A compilation of the ambient temperature tensile properties of the as-received copper–lead alloys is given in Table I. Duplicate samples were tested for each composition and no significant variation between the pairs of samples was observed.

The elastic modulus, $E$, obtained by extensometer trace, decreased with increasing lead content in the copper matrix. Increasing the lead content from 10 wt % (46.1 GPa) to 25 wt % (34.4 GPa) decreased the elastic modulus by 25 %. Further increase in lead content from 25 wt % (34.4 GPa) to 40 wt % (30.2 GPa) decreased the elastic modulus by only 12 %. The elastic modulus of the 6040 alloy (30.2 GPa) was 35 % lower than the 9010 counterpart (46.1 GPa). The variation of modulus with lead content is shown in Fig. 4.

The yield strength, $\sigma_{0.2}$, defined as the stress required at a plastic strain of 0.2 %, decreases with an increase in lead content. The yield strength of the 9010 alloy is 81 MPa. An increase in lead content from 10 wt % to 25 wt % decreased the yield strength by 28 %, and by 35 % for a further increase in lead content, that is, for the alloy with 40 wt % lead. The variation of ultimate tensile strength with lead content was similar to the variation of yield strength. The variation of strength with lead content (weight per cent), shown in Fig. 5, is observed to be non-linear. Lead is softer than copper and an increase in lead content softens the copper matrix, which is well reflected in the strength of the alloys.

Ductility measurements, obtained by tensile elongation over a gauge length of 12.7 mm, reveal the copper–lead alloys tested to possess acceptable ductility. The improvement in elongation, $\varepsilon_f$, was:

(i) 30 % for an increase in lead content from 10 wt % to 25 wt %, and

(ii) 96 % for an increase in lead content from 10 wt % to 40 wt %.

It is interesting to note that plastic strain, $\varepsilon_p$, accounts for in excess of 95 % of the tensile elongation, $\varepsilon_f$. This is clearly indicative of the ductile nature of the composite copper–lead matrix. The reduction in area, RA, another measure of tensile ductility:

(i) increased 25 % with increase in lead content from 10 wt % to 25 wt %, and

(ii) improved in excess of 150 % for increase in lead content to 40 wt %.

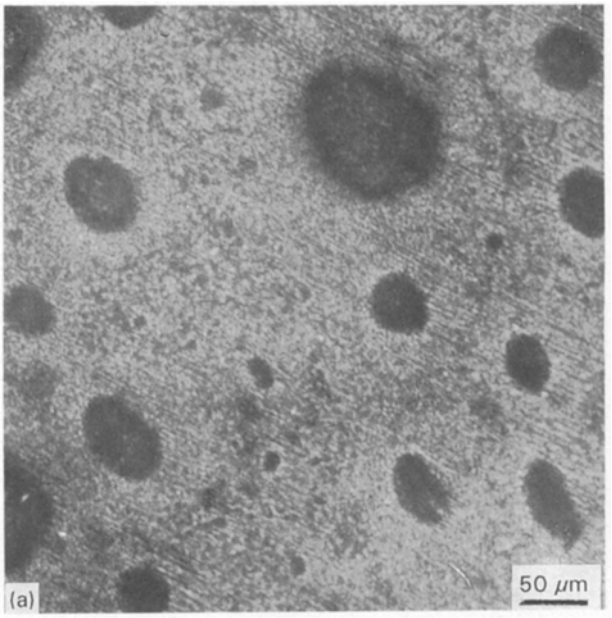


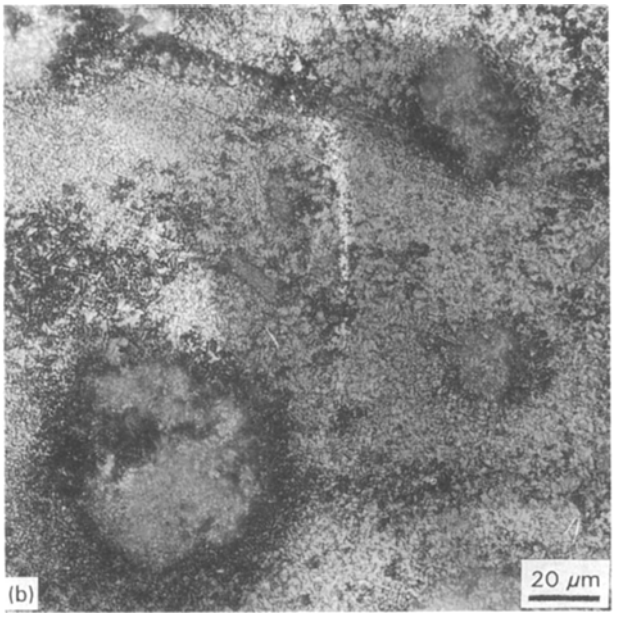


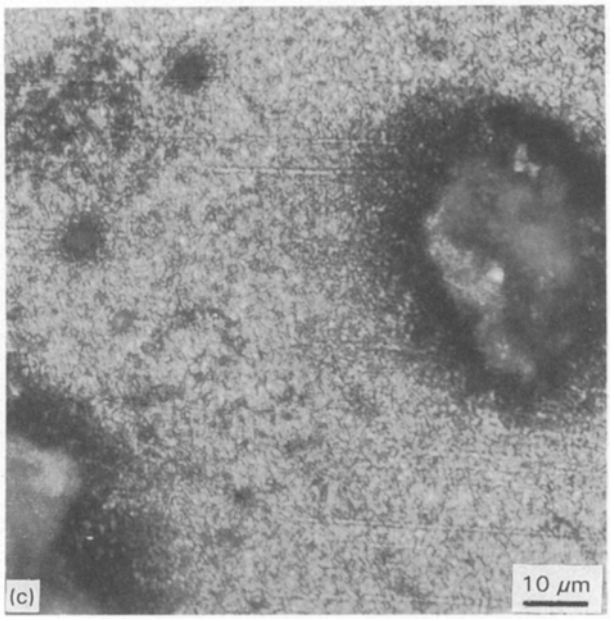


*Figure 3* Optical micrographs of the copper (60 wt %)–lead (40 wt %) alloy showing morphology and distribution of lead particles.

The variation of tensile elongation and reduction in area with lead content, shown in Fig. 6, is parabolic. The observed improvement in both elongation and reduction in area is consistent with the degradation in strength recorded with increasing lead content. A comparison of the engineering stress–engineering strain curves for the three alloys is provided in Fig. 7.

The observed decrease in strength of the alloys containing a high lead content is attributed to an increase in both the number and size of soft lead particles dispersed in the copper matrix. An increase in the number of lead globules (particles) results in a concurrent decrease in load-bearing capability of the material. Furthermore, the lead particles on account of their intrinsic softness deform easily, even at low values of far-field applied stress.

The strain-hardening characteristic of the alloys was evaluated from examining the variation of stress with plastic strain, plotted on a bilogarithmic scale (Fig. 8). The variation of stress, $\sigma$, with plastic strain, $\varepsilon_p$, obeyed a relationship of the form

$$\sigma = K(\varepsilon_p)^n \quad (1)$$

where $K$ is the monotonic strength coefficient and $n$ is the monotonic strain-hardening exponent. The strain-hardening exponent decreases with increasing lead content and conforms well with the loss in strength. The monotonic parameters $n$ and $K$ are summarized in Table II.

The tensile fracture surfaces are helpful in elucidating microstructural effects on ductility and fracture

TABLE I Room-temperature tensile properties of copper–lead alloys[a]

| Alloy | Elastic modulus, $E$[b] GPa(Msi) | 0.2 % yield stress (MPa) ($10^3$ p.s.i.) | UTS (MPa)($10^3$ p.s.i.) | Elongation (G.L. = 12.7 mm) (%) | Plastic strain to failure, $\varepsilon_p$ (%) | Tensile ductility, $\ln(A_0/A_f)$ | RA (%) |
|---|---|---|---|---|---|---|---|
| 90 Cu–10Pb | 46.1(6.7) | 80.9(11.7) | 118.4(17.2) | 8.21 | 8.13 | 0.03 | 3.3 |
| 75 Cu–25Pb | 34.4(5.0) | 58.6(8.5) | 83.6(12.1) | 10.66 | 10.58 | 0.04 | 4.1 |
| 60 Cu–40Pb | 30.2(4.4) | 52.6(7.6) | 78.0(11.3) | 16.12 | 16.07 | 0.09 | 8.5 |

[a] Results are mean based on two tests.
[b] Tangency measurements based on extensometer trace.

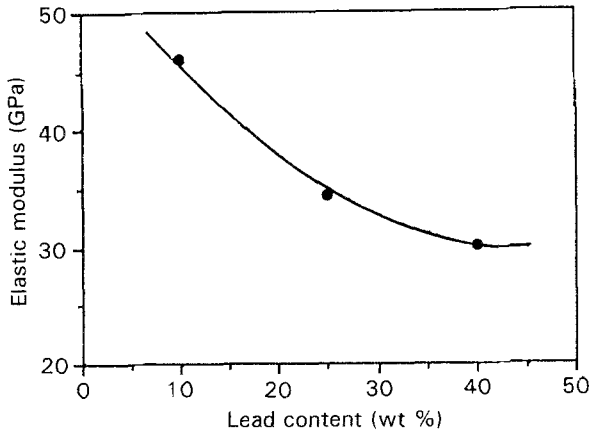


*Figure 4* Variation of elastic modulus with lead content.

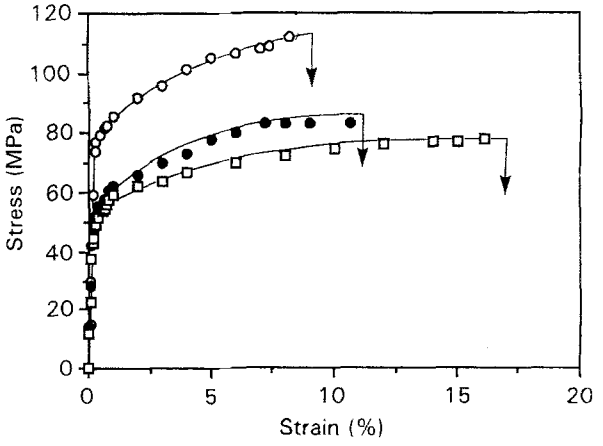


*Figure 7* Comparison of the engineering stress–engineering strain curves for the three alloys: (○) 9010, (●) 7525, (□) 6040.

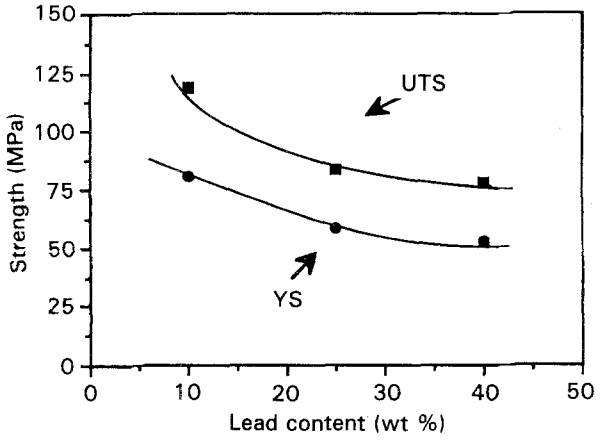


*Figure 5* Variation of strength of the alloys with lead content.

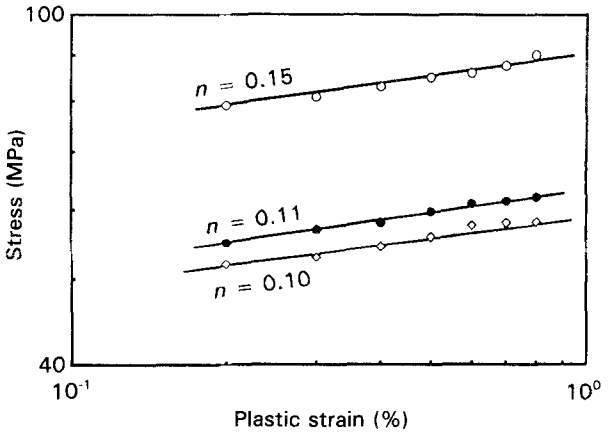


*Figure 8* Monotonic stress–strain curve for the copper–lead alloys: (○) 9010, (●) 7525, (□) 6040.

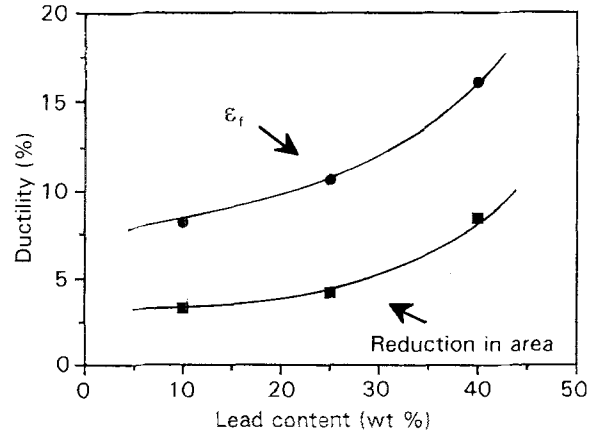


*Figure 6* Variation of tensile elongation and reduction in area with lead content.

TABLE II Monotonic parameters of copper–lead alloys

| Alloy | Strain-hardening exponent, $n$ | Strength coefficient, $K$ (MPa)($10^3$ p.s.i.) |
|---|---|---|
| 90Cu–10Pb | 0.15 | 88(12.8) |
| 75Cu–25Pb | 0.11 | 63(9.1) |
| 60Cu–40Pb | 0.10 | 57(8.3) |

properties of the alloy. Scanning electron microscope examination of the fracture surface features of the deformed tensile specimens was done at low magnification to identify the overall fracture morphology and at higher magnification to identify the fine-scale fracture features. Fractography of the tensile samples revealed near similar features for the three alloys. Representative fracture features for the three alloys are shown in Figs 9–11.

On a macroscopic scale, tensile fracture was predominantly transgranular with the formation of voids and shallow dimples. The voids result due to the conjoint action of the following two mechanisms.

(i) the removal of soft lead particles from the copper matrix during far-field tensile loading;

(ii) the development of a critical normal stress across the dispersed lead particle or matrix–particle interface.

On a macroscopic scale, tensile fracture of the 9010 alloy revealed a population of voids of a wide range of sizes. Examination of the fracture surface at high magnifications, revealed features reminiscent of a locally ductile mechanism. The microvoids were homogeneously distributed throughout the fracture surface and their near-equiaxed shape suggests that they nucleate around the inclusions (lead globules). Under the influence of far-field tensile stress, triaxial stresses are generated in the matrix and the voids appear to have undergone significant growth resulting in their forming an oval shape (Fig. 11b). At several locations the

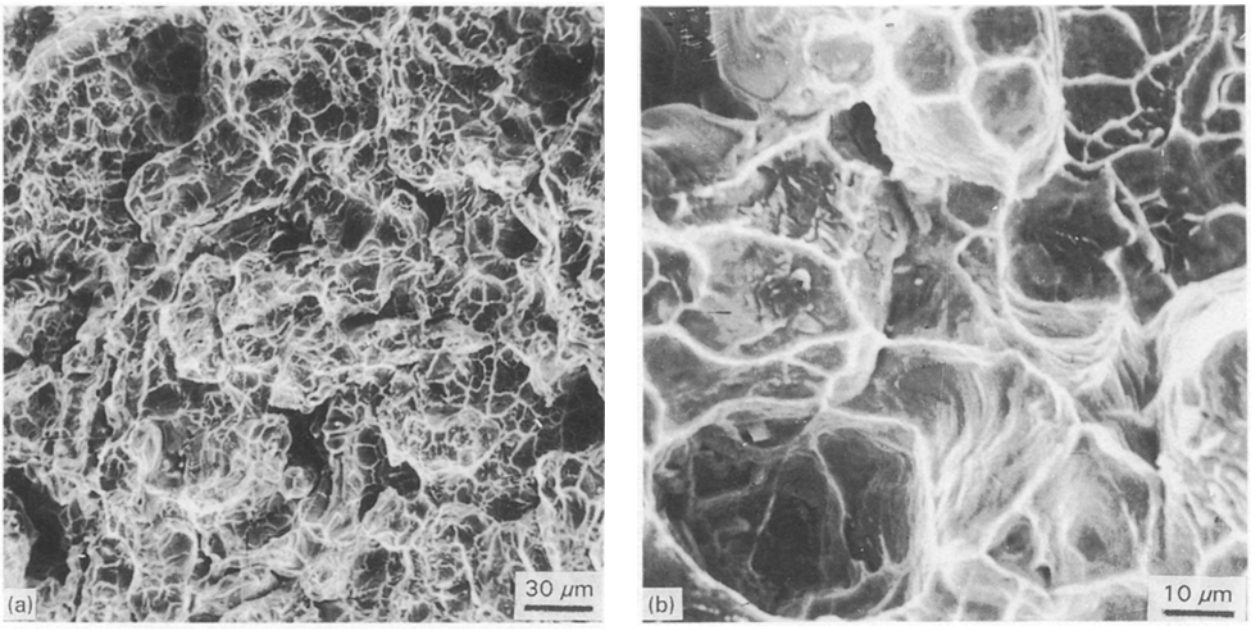


*Figure 9* Scanning electron micrographs of the tensile fracture surface of alloy 9010 showing (a) macroscopic and microscopic voids, (b) shallow near-equiaxed dimples, (c) lead particles on the fracture surface.

macroscopic voids were connected by a string of microscopic voids (Fig. 10a). Because crack extension under quasi-static loading occurs at high stress intensities, comparable to the quasi-static fracture toughness of the material, the presence of microvoids degrades the actual strain to failure associated with the ductile failure. The very fine microvoids coalesce and the halves of these voids are the dimples visible on the fracture surface (Fig. 12).

Fracture surface of the alloy with 25 wt % lead revealed pockets of lead globules (Fig. 10). High-magnification studies revealed failure at the matrix–particle interface with concurrent shearing of

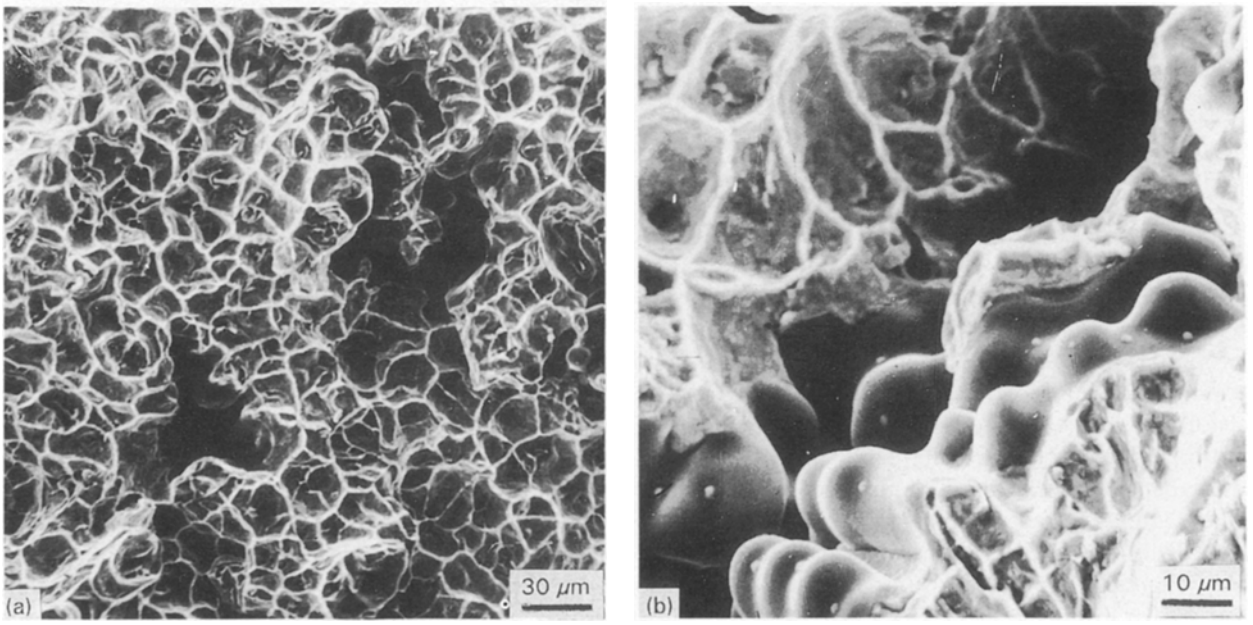


*Figure 10* Scanning electron micrographs of the tensile fracture surface of alloy 7525 showing (a) macroscopic voids and shallow dimples, (b) coalescence of microvoids to form a grain-boundary crack.

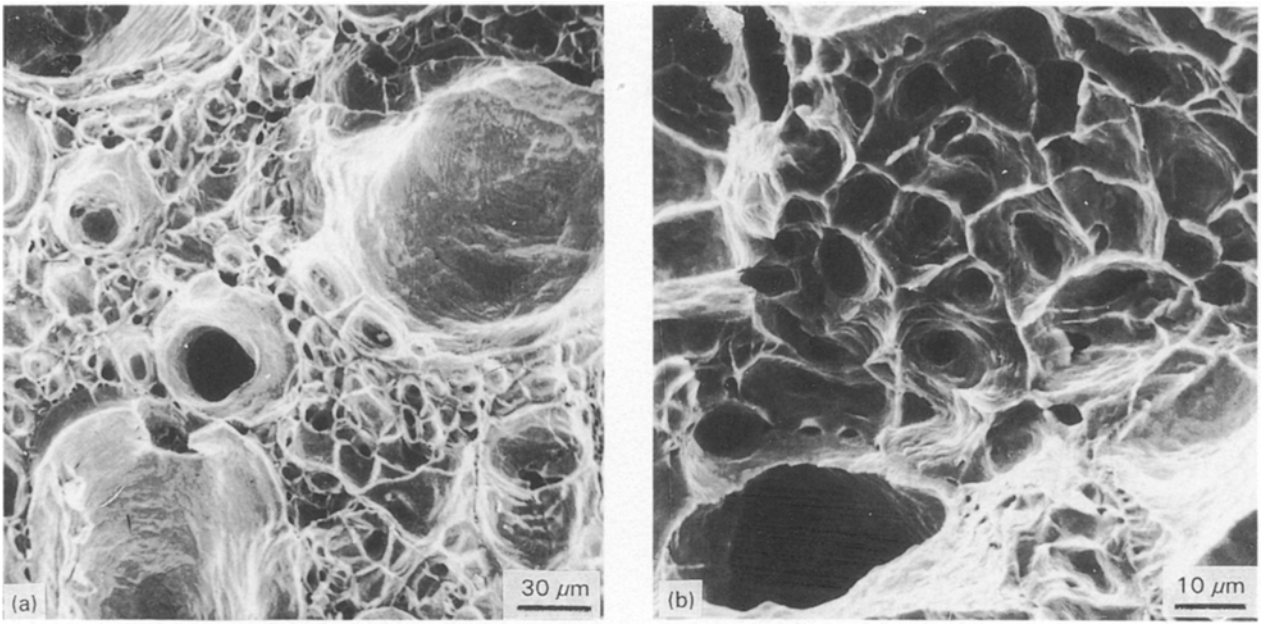


*Figure 11* Scanning electron micrographs of the tensile fracture surface of alloy 6040 showing (a) microscopic voids and shallow dimples, (b) growth of a void resulting in ovalization.

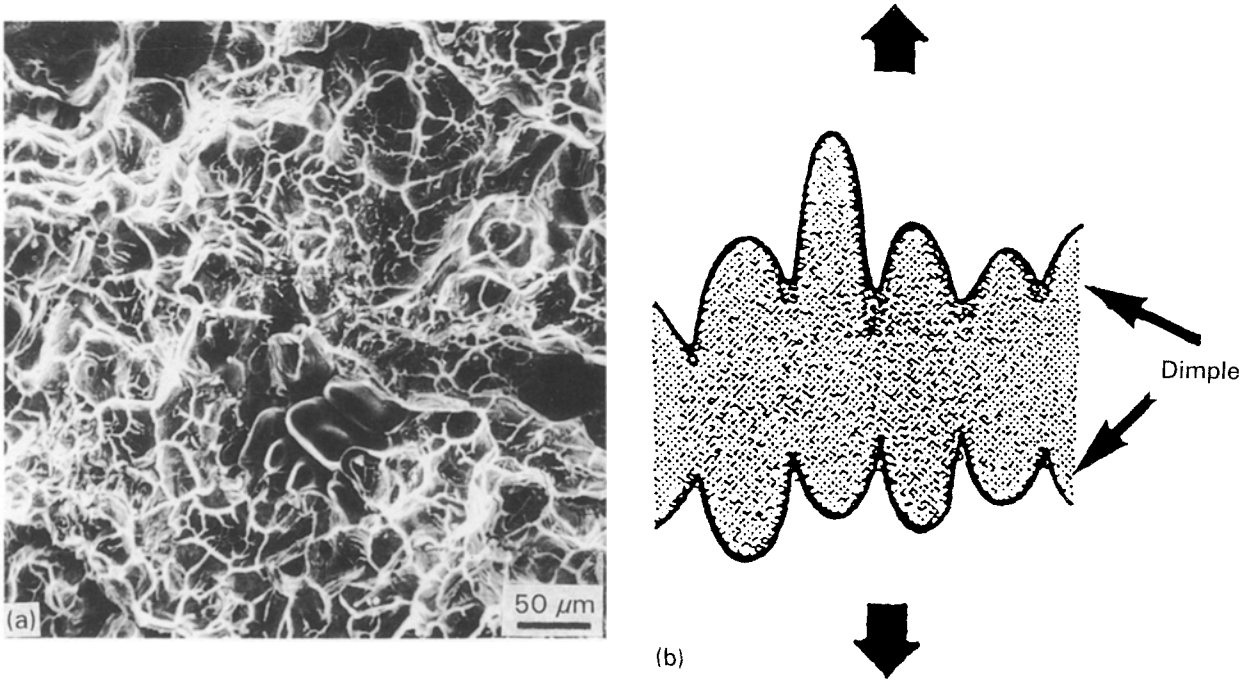


*Figure 12* (a) Scanning electron micrograph showing the presence of voids and shallow dimples on the fracture surface. (b) Schematic representation of dimples observed on the fracture surface.

the lead particles. The concentration of failure was more at the lead particles and not in the copper matrix. Low-magnification observations of the 6040 alloy revealed a large population of macroscopic voids of varying sizes (Fig. 11). Because the large lead particles were interdispersed with the smaller particles the fracture surface revealed a large population of smaller voids intermingled with the larger voids. At regular intervals clustering of both the macroscopic and microscopic voids was observed (Fig. 11b).

## 4. Conclusions

Based on a study of the influence of alloy composition on microstructure and tensile behaviour of copper-lead alloys, the following key observations were made.

1. The microstructure of the alloys consisted of particles or globules of lead dispersed randomly in the copper matrix. An increase in lead content resulted in an increase in both size and number of particles in the matrix.

2. The elastic modulus of the alloys decreases with an increase in lead content.

3. The strength (yield strength and ultimate tensile strength) of the alloy is dependent on lead content. An increase in lead content resulted in a decrease in strength. The strain-hardening capability of the alloy decreased with increased lead content.

4. Tensile elongation and reduction in area increased with an increase in lead content. The improvement is consistent with the degradation in strength resulting from increased lead content.

5. Tensile fracture of the alloys revealed features reminiscent of a locally ductile mechanism.

## Acknowledgement

This research was supported by the International Copper Association under Grant ICA: 143, Program Manager, Dr Nathan L. Church.

## References

1. J. D. LIVINGSTON and C. E. HENRY, *Trans. Metall. Soc. AIME* **245** (1969) 351.
2. T. S. SUDARSHAN, Final Report, Contract F33615-88-C-5493, Department of Air Force, Air Force Systems Command, Wright Patterson Air Force Base, OH (1989).
3. M. HANSEN and K. ANDERKO, Constitution of Binary Alloys, second edn (McGraw Hill, New York, 1958) p. 347.
4. J. D. LIVINGSTON and H. E. CLINE, *Trans. Metall. Soc. AIME* **245** (1969) 351.
5. S. SHAH, R. N. GRUGEL and B. D. LICHTER, *Metall. Trans.* **19A** (1988) 2677.
6. J. B. ANDREWS, A. C. SANDIA and P. A. CURRERI, *ibid.* **19A** (1988) 2645.
7. R. N. GRUGEL and A. HELLAWELL, *ibid.* **12A** (1981) 669.
8. T. S. SRIVATSAN, S. ANAND and T. S. SUDARSHAN, *Mater. Lett.* (1992) **13** (1992) 109–114.
9. S. ANAND, MSc thesis, University of Akron, May 1992.
10. S. ANAND, T. S. SRIVATSAN and T. S. SUDARSHAN, *Int. J. Fatigue* **15** (1993), in press.
11. A. DE LA TORRE, P. ADEVA and M. ABALLE, *J. Mater. Sci.* **26** (1991) 4351.

*Received 17 March 1992*
*and accepted 24 February 1993*